

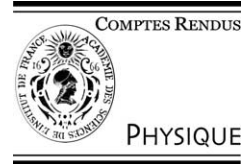


ELSEVIER

Available online at www.sciencedirect.com

SCIENCE @ DIRECT®

C. R. Physique 4 (2003) 823–832



The Cosmic Microwave Background/Le rayonnement fossile à 3K

CMB: A, B, C, . . . , W and beyond (P!)

François R. Bouchet

Institut d'astrophysique de Paris, CNRS, 98 bis, boulevard Arago, 75014 Paris, France

Presented by Guy Laval

Abstract

In this introductory note to the issue of the *Comptes Rendus Physique*, I describe the *ABC* of Cosmic Microwave Background (CMB) physics, which explains why high accuracy observations of the CMB spectrum and of its spatial structure are unique tools for the determination of the global cosmological parameters and for simultaneously constraining the physics of the early universe. I also briefly survey the many experiments, Archeops, Boomerang, COBE but also DASI, CBI, MAXIMA, . . . to name but a few, which have measured the anisotropies of the CMB and led to crucial advances in observational cosmology. The somewhat frantic series of new results has recently culminated with the outcome of the WMAP satellite, which confirmed earlier results, set new standards of accuracy, and suggested that the Universe may have re-ionised earlier than anticipated. Many more CMB experiments are currently taking data or being planned, with the Planck satellite on the 2007 Horizon poised to extract all the cosmological information in the temperature anisotropies, and foray deeply into polarisation. **To cite this article:** *F.R. Bouchet, C. R. Physique 4 (2003).*

© 2003 Académie des sciences. Published by Elsevier SAS. All rights reserved.

Résumé

Le CMB A, B, C, . . . , W et au-delà (P!). Dans cette note d'introduction pour le volume des *Comptes Rendus Physique*, je décris l'*ABC* de la physique du fond de rayonnement fossile à 3K (CMB) qui explique pourquoi les observations très précises du spectre du CMB ainsi que de sa structure spatiale constituent un outil unique pour déterminer les paramètres cosmologiques globaux et pour simultanément contraindre la physique de l'univers primordial. Puis, je rappelle succinctement les nombreuses expériences, Archeops, Boomerang, COBE mais aussi DASI, CBI, MAXIMA, . . . pour n'en nommer que quelques unes, qui ont mesuré les anisotropies du CMB et ont permis des avancées cruciales en cosmologie observationnelle. La série de nouveaux résultats à un rythme assez frénétique a récemment culminée avec le satellite WMAP qui a confirmé les mesures précédentes, établit de nouveaux standards de précision, et suggéré que l'Univers a pu être réionisé plus tôt que prévu. Beaucoup d'autres expériences sont en cours ou à venir, dont le satellite Planck à l'horizon 2007 qui devrait extraire des anisotropies de température toute l'information cosmologique utilisable, et apporter une contribution fondamentale à la mesure de la polarisation du CMB. **Pour citer cet article :** *F.R. Bouchet, C. R. Physique 4 (2003).*

© 2003 Académie des sciences. Published by Elsevier SAS. All rights reserved.

Keywords: Cosmic Microwave Background Anisotropies; Cosmology; Early Universe

Mots-clés : Anisotropies du fond de rayonnement cosmique ; Cosmologie ; Univers primordial

1. The cosmic background

The cosmic background is the present electromagnetic content of the universe averaged over a large volume. Observationally, it is defined as the isotropic background observed when one has removed the components radiated by our Galaxy or by the solar

E-mail address: bouchet@iap.fr (F.R. Bouchet).

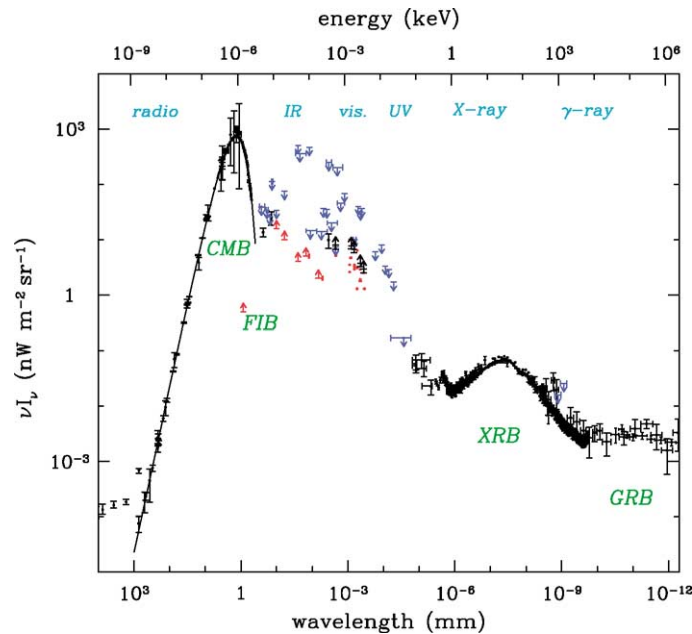


Fig. 1. Cosmic background spectrum from radio to gamma rays, as summarised by Halpern and Scott in 1999 [22]. The intensity is shown per logarithmic frequency interval, νI_ν , so that the energy in different bands can be directly compared. Reprinted from [22].

system and of course all instrumental straylight. The spectral energy distribution of this background is shown in Fig. 1; it is dominated by a microwave component which contains 93% of the energy. The CMB is the only one to be clearly diffuse and it has a spectrum very close to a Planck function. This shape was a definite prediction of the so-called Big Bang model with early predictions of the expected present temperature of about 5K [1] (see the review of the CMB isotropic component by Bouchet and Puget, this issue).

In this expanding model from a hot and dense phase, this Planckian shape was acquired very early, at a redshift $\gtrsim 10^7$, when reactions which do not conserve the photon number (bremsstrahlung, $e \rightarrow e\gamma$, double-Compton $e \rightarrow e\gamma\gamma$) froze out, i.e. when their characteristic times became larger than the expansion time ($H^{-1} = (\dot{a}/a)^{-1}$, if a stands for the scale factor of the metric). Later on, the photon distribution function kept constant but for a temperature decrease proportional to a . The FIRAS instrument aboard the COBE satellite measured the current temperature $T_0 = 2.725 \pm 0.001$ K [2] (yielding a number density of about 400 photons per cubic centimetre).

In the early universe, baryons and photons were tightly coupled through Thomson scatterings of photons by free electrons (and nuclei equilibrate collisionally with electrons). When the temperature in the universe becomes smaller than about 3000 K (which is much lower than 13.6 eV due to the large number of photons per baryons $\sim 1.5 \times 10^9$), the cosmic plasma recombines and the ionisation rate x_e falls from 1 at $z > 1100$ down to $x_e < 10^{-3}$ at $z < 1100$: the photons mean free path $\propto 1/x_e$ rapidly becomes much larger than the Horizon $\sim cH^{-1}$, which is the distance over which causal processes can operate. As a result, the universe becomes transparent to background photons, over a narrow redshift range of 200 or less. Photons will then propagate freely as long as galaxies and quasars do not reionise the universe (but by then the density will have fallen enough that only a small fraction of the CMB photons will be rescattered). We therefore observe a thin shell around us, the Last Scattering ‘Surface’ (LSS in short) where the overwhelming majority of photons last interacted with baryonic matter at a redshift of 1100, when the Universe was less than 400 000 years old.

2. Structuring the Universe...

As we shall see, the analysis of the CMB temperature anisotropies indicated that the total energy density of the Universe is quite close to the so-called critical density, ρ_c , or equivalently $\Omega = \rho/\rho_c \simeq 1$. We therefore live in a close-to-spatially flat Universe. In agreement with the indications of other cosmological probes, the recent results of the CMB satellite WMAP [3] indicate that about 1/3 of that density appear to be contributed by matter ($\Omega_M = 0.29 \pm 0.07$), most of which is dark – i.e. not interacting electromagnetically – and cold – i.e. its primordial velocity dispersion can be neglected. The usual atoms (the baryons) contribute less than about 5% ($\Omega_B \simeq 0.047 \pm 0.006$) [4]. If present, a hot dark matter component (like massive

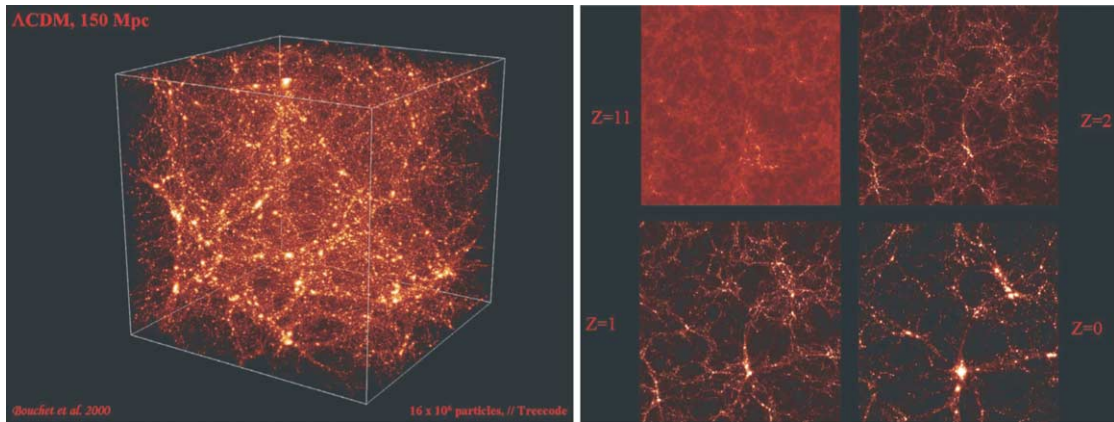


Fig. 2. A numerical simulation in a 150 Mpc box of a LCDM Universe ($\Omega = 1$, $\Omega_\Lambda = 2/3$, $n_S = 1$). (a) (left) Resulting distribution of the CDM at present (luminosity proportional to the density). (b) (right) Temporal evolution by gravitational instability of a thin (15 Mpc) slice of the box. It shows the hierarchical development of structures within a global cosmic web of increasing contrast, but quite discernible early on.

neutrinos) does not play a significant role in determining the global evolution of the Universe. While many candidate particles have been proposed for this CDM, it has not yet been detected in laboratory experiments, although the sensitivities of the latter are now reaching the range where realistic candidates may lay. The other $\sim 60\%$ of the critical density is contributed by a smoothly distributed vacuum energy density or dark energy, whose net effect is repulsive, i.e. it tends to accelerate the expansion of the Universe. Alternatively, this effect might arise from the presence in Einstein's equation of the famous cosmological constant term, Λ . While this global census, surprising as it may be, had been around already for some time (see Section 5), the WMAP results have tightened earlier constraints and gave further confidence to the model.

The spatial distribution of galaxies revealed the existence of large scale structures (clusters of size ~ 5 Mpc, filaments connecting them, and voids of size ~ 50 Mpc), whose existence and statistical properties can be accounted for by the development of primordial fluctuations by gravitational instability. The current paradigm is that these fluctuations were generated in the very early Universe, probably during an inflationary period; that they evolved linearly during a long period, and more recently reached density contrasts high enough to form bound objects. Given the census given above, the dominant component that can cluster gravitationally is Cold Dark Matter (CDM).

The analysis of the CMB anisotropies also indicate that the initial fluctuation statistics had no large deviations from a Gaussian distribution and that they were mostly adiabatic, i.e. all components (CDM, baryons, photons) had the same spatial distribution. The power spectrum of the initial conditions appears to be closely approximated by a power law $P(k) = \langle \delta_k^2 \rangle = A_S k^{n_S}$, where δ_k stands for the Fourier transform of the density contrast ($P(k)$ is therefore the Fourier transform of the two-point spatial correlation function). The logarithmic slope, n_S , is quite close to unity ($n_S = 0.99 \pm 0.04$ from WMAP alone [4]). This shape implies that small scales collapsed first, followed by larger scales, with small objects merging to form bigger objects. The formation of structures thus appear to proceed *hierarchically* within a 'cosmic web' of larger structures of contrast increasing with time.

Fig. 2(a) shows the generated structures in the CDM components in a numerical simulation box of 150 Mpc, while Fig. 2(b) shows the evolution with redshift of the density in a thin slice of that box. The statistical properties of the derived distribution (with the cosmological parameters given above) appear to provide a close match to those derived from large galaxy surveys. Note that we performed this simulation with $\Omega_\Lambda = 2/3$, $\Omega_M = 1/3$ in 2000, well before the WMAP results of 2002. Indeed, it was already by then the favourite model.

When collapsed objects are formed, the baryonic gas initially follows the infall. However, shocks will heat that gas, which can later settle in a disk and cool, and form stars and black holes which can then feed back through ionising photons, winds, supernovae... on the evolution of the remaining gas (after first re-ionising the Universe at $z > 6$). In this picture, galaxies are therefore (possibly biased) tracers of the underlying large scale structures of the dark matter. This picture has had considerable success, and a few shortfalls which concentrate much current cosmological activity...

3. ABC of CMB anisotropies

In this standard cosmological model, processes in the very early universe generated the seed fluctuations which give rise to all the structures we see today through the development of gravitational instability. Inflation is a class of mechanisms which

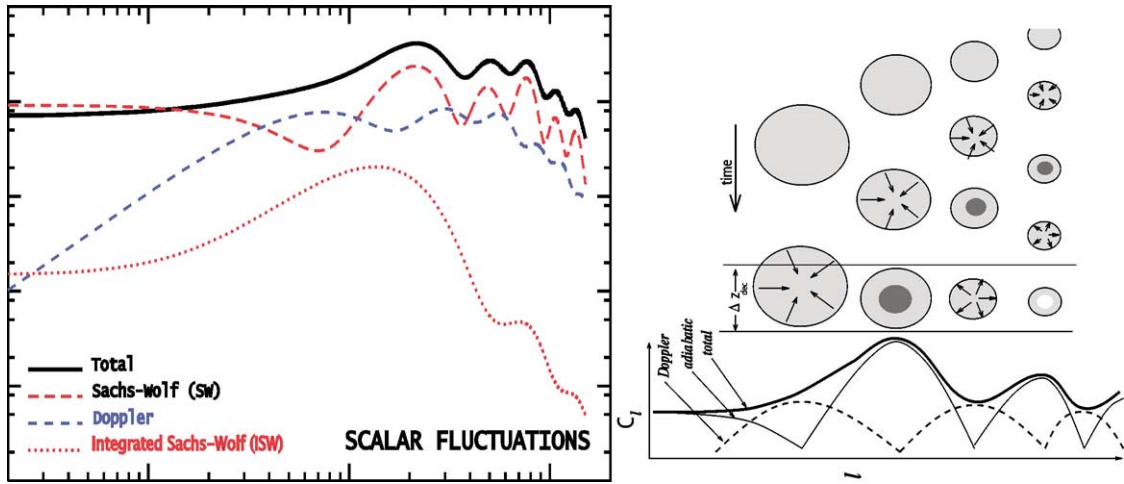


Fig. 3. The expected shape of the angular power spectrum of the temperature anisotropies, $C(\ell)$ (times ℓ^2 to give the logarithmic contribution of each scale to the variance). (a) Relative contributions; it has been assumed that only scalar fluctuations are present. The plot is in log-log coordinates. (b) As time progresses, larger and larger fluctuations start oscillating and leave their characteristic imprint on the spectrum (reprinted from [23]).

can bring quantum fluctuations to macroscopic scales (see the review by Parentani, this issue). Phase transitions in the early universe can also generate topological defects which contribute to the generation of fluctuations. Nevertheless, the present CMB anisotropies data do not allow these to be the dominant source for structure formation. The evolution of primordial fluctuations can be accurately followed and it was long predicted that to account for the formation of large scale structure their imprint as temperature fluctuations should have an rms of $\sim 100 \mu\text{K}$ (when CDM is present, which is indeed why it took so long to detect fluctuations that small).

To analyse the statistical properties of the temperature anisotropies, we can either compute the angular correlation function of the temperature contrast δ_T , or the angular power spectrum $C(\ell)$ which is its spherical harmonics transform. In practice, one transforms the δ_T pattern in $a(\ell, m)$ modes and sums over m at each multipole since the pattern should be isotropic, at least for the trivial topology (see however, Uzan and Riazuelo, this issue). A given multipole corresponds to an angular scale $\theta \sim 180^\circ/\ell$. These two-point statistics characterise completely a Gaussian field. Fig. 3(a) shows the expected $C(\ell)$ shape in the context we have described above.

This specific shape of the $C(\ell)$ arises from the interplay of several phenomena. One is the so-called ‘Sachs–Wolf effect’ [5] which is the energy loss of photons which must ‘climb out’ of potential well at the LSS (to ultimately reach us to be observed), an effect which superimposes to the intrinsic temperature fluctuations. Fig. 3(b) gives a pictorial view of the development of fluctuations. Since the density contrasts of these (scalar) fluctuations is very weak, one can perform a linear analysis and study each Fourier mode independently (the effect of the primordial spectrum is thus simply to weight the various modes in the final $C(\ell)$). Fig. 4 shows the (approximate) temporal evolution of the amplitude of different Fourier modes. While gravity tends to enhance the contrast, the (mostly photonic) pressure resists and at some point stops the collapse which bounces back, and expands before recollapsing again. . . This leads to acoustic oscillations, on scales small enough that the pressure can be effective, i.e. for $k > k_A$, where the acoustic scale k_A is set by the inverse of the distance travelled at the sound speed at the time η_* considered. On scales larger than the sound horizon ($k < k_A \propto 1/(c_S \eta_*)$), the initial contrast is simply amplified. At $k = k_A$ the amplification is maximal, while at $k = 2k_A$ it had time to fully bounce back. More generally, the odd-multiples of k_A are at maximal compression, while it is the opposite for the even multiples of k_A .

One should note the displacement of the zero point of the oscillations which results from the inertia that baryons bring to the fluid. The rms of the modes amplitude (right plot of Fig. 4) therefore show a relative enhancement of the odd (compression) peaks versus the even (rarefaction) ones, this enhancement being directly proportional to the quantity of baryons, i.e. $\Omega_B h^2$, if h stands for the Hubble ‘constant’, $H = \dot{a}/a$, in units of 100 km/s/Mpc (today $h_0 = 0.72 \pm 0.05$). Note that since Ω_X stands for the ratio of the density of X to the critical density (such that the Universe is spatially flat), and since that critical density decrease with time as h^{-2} , $\Omega_X h^2$ is indeed proportional to the physical density of X .

Let us assume that the LSS transition from opaque to transparent is instantaneous, at $\eta = \eta_*$. What we would see then should just be the direct image of these standing waves on the LSS; one therefore expects a series of peak at multipoles $\ell_A = k_A \times D_*$, where D_* is the angular distance to the LSS, which depends on the geometry of the spacetime. Of course a given k contributes to some range in ℓ (when k is perpendicular to the line of sight, it contributes to lower ℓ than when the angle decreases), but

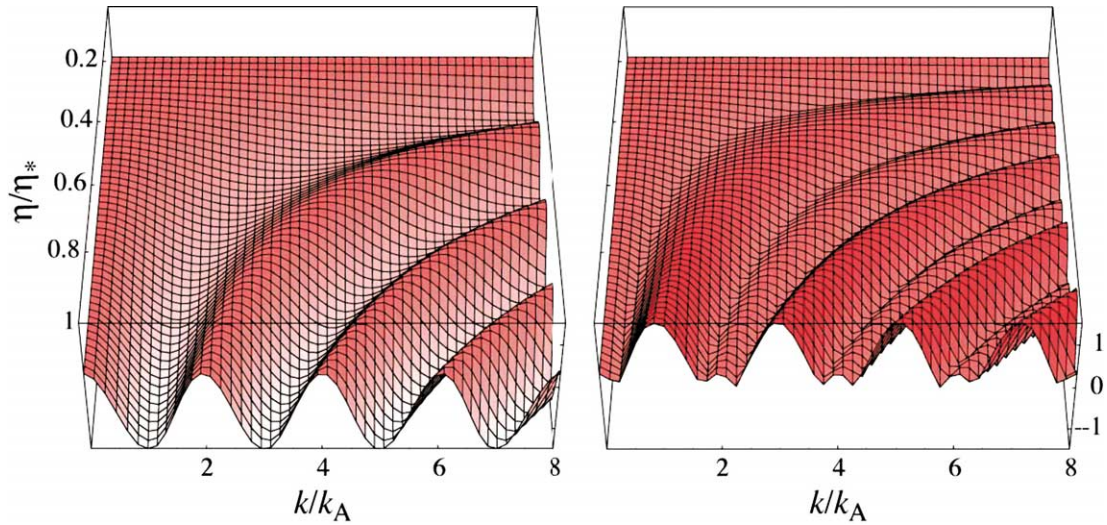


Fig. 4. Temporal evolution of the effective temperature which sums the effects (of opposite sign) of the intrinsic temperature and of the Newtonian potential fluctuations (for $R = (p_B + \rho_B)/(p_\gamma + \rho_\gamma) = \text{cste}$). (a) (left) Amplitude. Note the zero point displacement which leads to a relative enhancement of compressions. (b) (right) rms showing the enhanced odd-numbered peaks. Reprinted from [6], with permission from Elsevier.

this smearing is rather limited. The dependence of the acoustic angular scale ℓ_A on geometry and sound speed leads to its dependence on the values of three cosmological parameters. One finds for instance

$$\frac{\Delta \ell_A}{\ell_A} \simeq -1.1 \frac{\Delta \Omega}{\Omega} - 0.24 \frac{\Delta \Omega_M h^2}{\Omega_M h^2} + 0.07 \frac{\Delta \Omega_B h^2}{\Omega_B h^2} \quad (1)$$

around a flat model $\Omega = 1$ with 15% of matter ($\Omega_M h^2 = 0.15$) and 2% of baryons [6]. Note that this information on the peaks positions (and in particular that of the first one) is mostly dependent on the total value of Ω (geometry), with some weaker dependence on the matter content $\Omega_M h^2$.

As mentioned earlier, the baryons increase the inertia of the baryon–photon fluid and shifts the zero point of the oscillations. A larger baryonic density tends to increase the contrast between odd and even peaks; one can therefore use this contrast-in-height information to learn about the baryonic density. The influence of dark matter is more subtle. At very early times, the dominant energy density is that of radiation. But the energy density of matter decreases more slowly, $\propto a^{-3}$, than that of radiation, $\propto a^{-4}$ (the ‘stretching’ of the photon wavelength with expansion brings in another factor of a to the volume dilution effect felt by matter). Therefore more matter means an earlier transition from radiation to matter domination. The current consensus is that this transition happens at $z_{\text{eq}} = 3454_{-392}^{+385}$ [4], shortly before recombination. The decay of the gravitational potential of modes oscillating in the radiation era boosts the amplitudes of the modes which started oscillating in that era, i.e. those with $k > k_{\text{boost}}$ which is $\gtrsim k_A$ for this value of z_{eq} . An earlier transition means an increase in k_{boost} , i.e. only larger k modes are boosted. The net effect is to globally *decrease* the peak amplitude when the matter content increases (in addition to the small shift in scale due to the variation of ℓ_A already noted above). The effect on the power spectrum peaks of all the matter is thus rather different from that of the baryonic component alone. Therefore the shape of the spectrum is sensitive to both separately. This suggests that degeneracies in the effect of these three parameters ($\Omega, \Omega_M, \Omega_B$) can be lifted with sufficiently accurate CMB measurements.

Since the fluid is oscillating, there is also a *Doppler effect* in the k direction (blue dotted line in Fig. 3(a), which is zero at the acoustic peaks and maximal in between. This effect adds in quadrature to the Sachs–Wolf effect considered so far. Indeed, if we imagine an acoustic wave with k perpendicular to the line of sight, we see no Doppler effect, while for a k parallel to the line of sight, the Doppler effect is maximal and the Sachs–Wolf effect is null. This smoothes out the peak and trough structure, although not completely since the Doppler effect is somewhat weaker than the SW effect (by an amount $\propto \Omega_B h^2$). Therefore an increase in the baryonic abundance also increases the peak–trough contrast (in addition to the odd–even peak contrast).

So far we have considered the fluid as perfect and the transition to transparency as instantaneous, none of which is exactly true. Photons scattered by electrons through Thomson scattering in the baryons–photons fluid perform a random walk and diffuse away proportionally to the square root of time (in comoving coordinates which remove the effect of expansion). Being more numerous than the electrons by a factor of a few billion, they drag the electrons with them (which by collisions drag in

turn the protons). Therefore all fluctuations smaller than the diffusion scale are severely dampened. This so-called Silk damping is enhanced by the rapid increase of this diffusion scale during the rapid but not instantaneous combination of electrons and protons which leads to the transparency. As a result of the finite thickness of the LSS and the imperfection of the fluid, there is an exponential cut-off of the large- ℓ part of the angular power spectrum. There is therefore not much primordial pattern to observe at scales smaller than $\sim 5'$.

After recombination, photons must travel through the developing large scale structures to reach the observer. They can lose energy by having to climb out of potential well which are deeper than when they fell in (depending on the rate of growth of structures, which depends in turn on the cosmological census). Of course the reciprocal is also true, i.e. they can gain energy from forming voids. These tend to cancel at small scale since the observer only sees the integrated effect along the line of sight. The red dotted line of Fig. 3 shows the typical shape of that *Integrated Sachs–Wolf* (ISW) contribution. The ISW is anti-correlated with the Sachs–Wolf effect, so that the total power spectrum $C(\ell)$ is in fact a bit smaller than the spectrum of each taken separately. Finally, other small secondary fluctuations might also leave their imprint, like the lensing of the LSS pattern by the intervening structures, which smoothes slightly the spectrum. However, that can be predicted accurately too. And in fact the smoothing kernel dependence on cosmological parameters introduces small effects that may help reducing some residual degeneracies between the effect of parameters on the power spectrum shape.

4. Complications

Other secondary effects, imprinted after recombination, are generally much weaker (at scales $> 5'$). For instance, the *Rees–Sciama* effect [7] (a non-linear version of the ISW) generates temperature fluctuations, with amplitudes of about a few 10^{-7} to 10^{-6} ; its amplitude is maximum for scales between 10 and 40 arc minutes [8]. At the degree scale, this contribution is only of the order of 0.01 to 0.1% of the primary CMB power. The inverse Compton scattering of the CMB photons on the free electrons of hot intra-cluster gas produces the *Sunyaev–Zel’dovich* (SZ) effect [9–11]. This effect has a specific spectral signature which should allow separating it, at least in a sufficiently sensitive multi-frequency experiment. But the motion along the line of sight of clusters induces a first order Doppler effect, usually called the *Kinetic Sunyaev–Zel’dovich* effect, which is a true source of temperature fluctuation, albeit rather weak (the rms cluster velocity is $\sim 10^{-3}c$) and in the specific direction of clusters. A similar effect, the *Ostriker–Vishniac effect* [12,13] arises from the correlations of the density and velocity perturbations along the line of sight, when the universe is totally ionised. The corresponding anisotropies are at the few arc-minute scale and their amplitudes depend much on the ionisation history of the universe [14,15]. However, they remain smaller than the primary anisotropies for $\ell < 2000$. This type of Doppler effect can in fact happen in all sorts of objects containing ionised gas, like expanding shells around the sources that reionised the Universe [16–19], or primordial galaxies hosting super-massive black holes [20], but the relevant angular scales are rather in the arc second range or smaller. This does not hold true, however, for various foreground emission, like those of our own Galaxy (see the review by Giard and Lagache, this issue). But, as for the Sunyaev–Zel’dovich effect, one can use multi-frequency observations to separate them out rather well. The note by Lagache and Aghanim (this issue) provides a review of these secondary effects and foregrounds. The note by Bouchet, Piat and Lamarre (this issue) shows the expected residuals of the component separation for the WMAP and Planck satellites.

Until now, we only considered scalar fluctuations. Vectorial perturbations tend to decay with expansion and are not predicted to leave any imprint on the spectrum. But it is anticipated that the very same process that generated the primordial scalar fluctuations also created a stochastic background of gravity waves. This weak tensorial contribution only appears in the low- ℓ part of the spectrum, before the first peak (since these waves decay as soon as their wavelength becomes smaller than the horizon, which roughly corresponds in ℓ to the first peak). At the current level of experimental precision it is most often ignored. However, this contribution is much more significant for the polarised part of the emission. Indeed, it is expected that the CMB fluctuations will be slightly polarised (see the review by Kaplan et al. in this issue).

Thomson scatterings can create polarisation provided the incident radiation is not isotropic, which can be induced by velocity gradients in the baryon–photon fluid. Before recombination, successive scatterings destroy the build up of any polarisation. One therefore anticipates a small degree of polarisation created at recombination, partially correlated with the temperature anisotropies (the velocity part of it). The degree of polarisation predicted for the CMB is of the order of 10%. Polarisation measurements of the CMB can therefore check the internal consistency of the measurements and help further removing degeneracies, like that between n_S , the logarithmic slope of the scalar initial spectrum and τ , the optical depth to LSS (which controls the exponential cutoff of the $C(\ell)$ and can mimic the tilt of the spectrum produced by changing n_S).

More importantly, polarisation measurements (see the review by Delabrouille et al., this issue) will provide the best way to constrain the tensor to scalar ratio, $r = A_S/A_T$ (of the normalisations of the primordial perturbations spectra). They may further lead to checking the consistency relation between r and the logarithmic slope of the gravitational wave power spectrum, n_T , which is predicted for inflation. Currently we can only say that $r < 0.71$ at 95% confidence limit [4], if only CMB data with no further priors are used, with essentially no constraint on n_T , but the data will undoubtedly continue to improve.

So far we concentrated on the case of adiabatic perturbations which develop under their own gravity when they are much larger than the sound horizon. After they enter this horizon, they become gravitationally stable and oscillate till the Universe becomes transparent. All perturbations of the same scale are in phase as they were all laid down and started to develop at the same time. These will lead to the so-called acoustic peaks in the resulting CMB power spectrum. In the case of active source of fluctuations such as in defects theories, perturbations are laid down at all times, they are generically isocurvature and non-Gaussian (see the review by Langlois, this issue), and the phases of the perturbations of a given scale are incoherent, which does not lead to many oscillation like in the coherent (e.g., inflationary) case. A single broad peak is expected, and this is why current CMB anisotropy data already indicates that defects cannot be a major source of CMB fluctuations and hence cannot seed by themselves the growth of the large scale structures of the Universe.

In summary, *the seeds of large scale structures must have left an imprint on the CMB, and the statistical characteristics of that imprint can be precisely predicted as a function of the properties of the primordial fluctuations and of the homogeneous Universe.* Reciprocally, we can use measurements of the anisotropies to constrain those properties.

5. Observations of CMB anisotropies

Many locations have been considered for CMB observations: ground-based telescopes at many places in the world, included at the South Pole, air-planes, stratospheric balloons, satellites around the Earth, and satellites far from the Earth. The main parameters related to the location are the atmospheric absorption and emission and the proximity of sources of straylight. The Earth's atmosphere is a very strong source at millimetre and submillimetre wavelengths [21]. It is therefore a source of photon noise. In addition, it is not perfectly uniform and the slowly changing structure of its emission adds noise that can be confused with CMB anisotropies. Even at stratospheric balloon altitudes (35 to 40 km), one may encounter structures at low angular frequencies that limit measurement stability. Only satellites are free of this first 'layer' of spurious emission.

Straylight coming from the Earth is a common problem for all locations except for space probes distant from the Earth as seen from the instrument. The brightness temperature of about 250 K of the Earth times its solid angle has to be compared with the instrument sensitivity in brightness times the beam solid angle. For a mission in low Earth orbit the ratio is 6×10^{13} and at the L2 Lagrange point the ratio is 5×10^9 , at the wavelengths of interest, diffraction is a major source of straylight, and modelling and experimentation can hardly estimate reliably or measure the very low side lobes needed to meet this extremely high rejection ratio. The problem is severe enough to have motivated the choice of the Lagrangian point L2 of the Sun–Earth system, at about 1.5 million kilometres from Earth, to locate the new generation of satellites WMAP and Planck.

The first clear detection of the CMB anisotropies was made in 1992 by the DMR instrument aboard the earth-orbiting COBE satellite (and soon afterwards by FIRS), with a ten degree (effective) beam and a signal to noise per pixel around 1. This led to a clear detection of the large scale, low- ℓ , Sachs–Wolf effect. The flatness of the curve (see Fig. 5(a)) indicated that the logarithmic slope of the primordial power spectrum, n_s , could not be far from one. The $\sim 30 \mu\text{K}$ height of the plateau gave a direct estimate of the normalisation of the spectrum, A_S (assuming the simplest theoretical framework, without much possible direct checks of the other predictions given the data).

In the next four years (Fig. 5(a)), a number of experiments started to suggest an increase of power around the degree scale, i.e. at $\ell \sim 200$. As shown by Fig. 5(b), by 1999 there was clear indication by many experiments taken together that a first peak had been detected. However, neither the height nor the location of that peak could be determined precisely, in particular in view of the relative calibration uncertainties (and possible residual systematics errors).

That situation changed in May 2000 when the BOOMERanG and MAXIMA (see Stompor et al., this issue) collaborations both announced a rather precise detection of the power spectrum from $\ell \sim 50$ to $\ell \gtrsim 600$. That brought a clear determination of the first peak around an ℓ of 220 (see panel (c)), with the immediate implications that Ω had to be close to one. This result had considerable resonance since it clearly indicated, after decades of intensive work, that the spatial geometry of the Universe is close to flat, with of course the imprecision due to the poor determination of the other parameters which also have an influence, albeit weaker, on the position of that peak (see Eq. (1)).

As recalled earlier, a crucial prediction of the simplest adiabatic scenario is the existence of a series of acoustic peaks whose relative contrast between the odd and even ones gives a rather direct handle on the baryonic abundance. In addition, one expects to see at larger ℓ the damping tail. All of these have now been established by the DASI 2001 experiment, an improved analysis of BOOMERanG, and by the release in May of this year of the VSA and CBI results. In addition the Archeops experiment gave at the end of 2002 a quite precise determination of the low- ℓ part of the spectrum (see Hamilton, Benoit et al. in this issue). Panel (d) of Fig. 5 shows a co-analysis performed by Bond of all results obtained till the end of 2002, as well as the recent determination by the WMAP satellite. Clearly, all the pre-WMAP sub-orbital experiments had done quite a wonderful job at pinning down the global shape of the temperature spectra. This panel also shows the spectrum as we know it today, when all experimental results are analysed together.

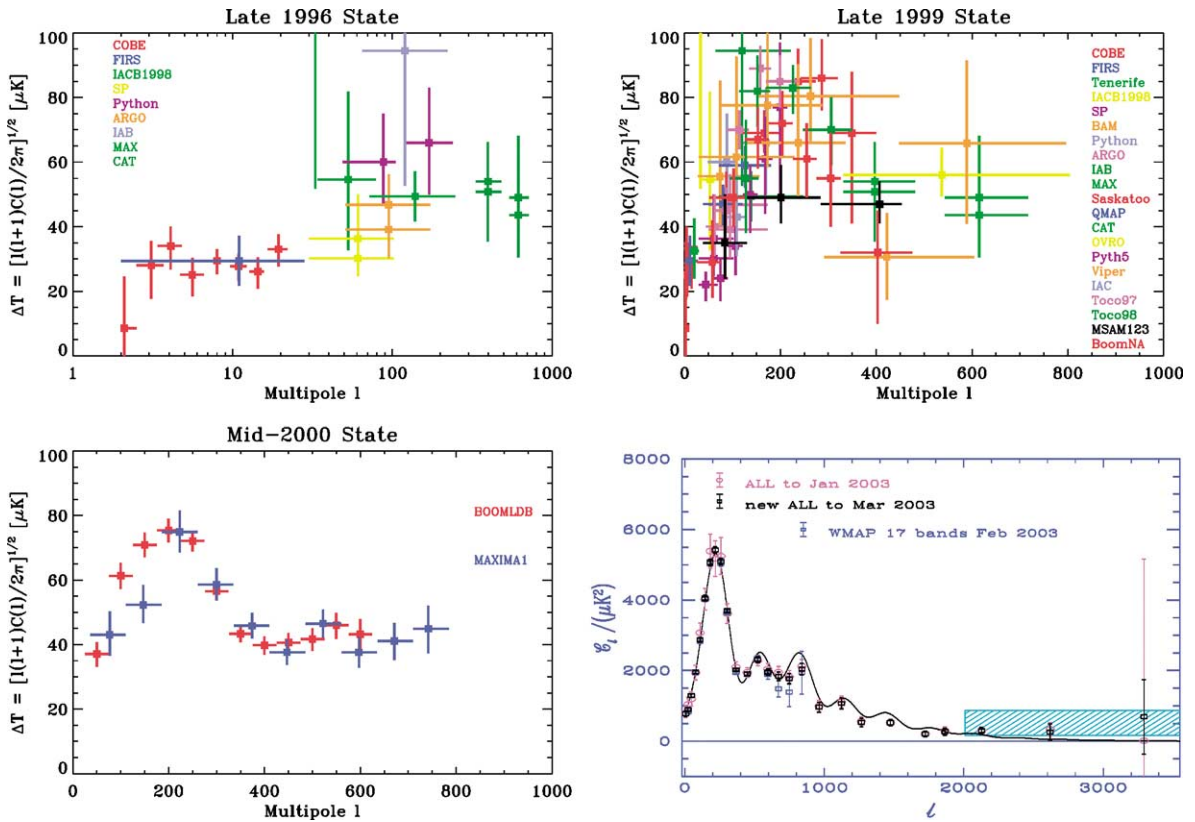


Fig. 5. Successive Measurements of the power spectrum. The first panel at top left shows all published detection at the end of 1996, while the second plot at right is an update at the end of 1999. The left bottom plot shows the two results published in May 2000 by the BOOMERanG and MAXIMA teams (with each curve moved by + or -1σ of their respective calibration). The final panel at bottom left (courtesy D. Bond) shows in purple the optimal spectra in 26 bands (allowing for calibration errors in each experiment) from the co-analysis of all data (including Archeops, the extended VSA, ACBAR and a preliminary version of the 2 year CBI data) until January 2003, as well as the WMAP spectrum (blue points), and the spectrum as we know it today (black points) when all experimental evidence are used.

Fig. 6 shows the constraints successively posed by these CMB experiments on some of the parameters of the model, using only weak priors arising from other cosmological studies (see a review by Douspis, this issue). These priors state that the current Hubble ‘constant’, $H_0 = 100h \text{ km/s/Mpc} \simeq h/(10^{10} \text{ yr})$, has to have a value between 45 and 90 km/s/Mpc, that the age of the Universe has to be greater than 10 billion years and that the matter density is larger than 1/10 of the critical density, all of which can be considered as very well established (if for instance the Universe has to be older than its oldest stars!).

The top left panel shows that indeed the curvature term $\Omega_k = 1 - \Omega$ has to be close to zero. The panel on the right shows that Ω_Λ and $\omega_c = \Omega_{CDM}h^2$ are not well determined independently of each other by single experiments. This simply reflects the fact that the $C(\ell)$ global pattern scales by the angular distance (recall $\ell_A = k_A D_*$) which is determined by the geometry (i.e., $\Omega = \Omega_\Lambda + \Omega_{CDM} (+\Omega_B)$), while the data is not precise enough to uncover the subtler effects which break that degeneracy. However, this degeneracy was lifted by the co-analysis of all experiments, even before WMAP, and independently of the supernovae result (see also the discussion by Blanchard, Bartlett and Douspis, this issue)...

The bottom left panel lends support to the $n_s = 1$ hypothesis. Many inflationary models suggest value of n_s slightly lower than one (and even departures from a pure power law), but the data is not yet good enough to address these questions convincingly. Completing the review, the bottom right shows the contours in the $\omega_b - \omega_c$ plane. The CMB determination turns out to be in excellent agreement with the constraints from primordial nucleosynthesis calculations which yield $\omega_b = \Omega_B h^2 = 0.019 \pm 0.002$.

In summary, this shows that many of the theoretical predictions corresponding to the simplest scenario for the generation of initial conditions (Gaussian statistics, adiabatic modes, no tensorial contribution, a scale invariant power spectrum) in a flat Universe dominated by dark energy and cold dark matter have now been detected, from the Sachs–Wolf plateau, to the series of peaks starting at $\ell \simeq 220$, to the damping tail, together with a first detection of the CMB polarisation at the expected level. The derived parameters are consistent with the various constraints from other cosmological probes and there are no glaring

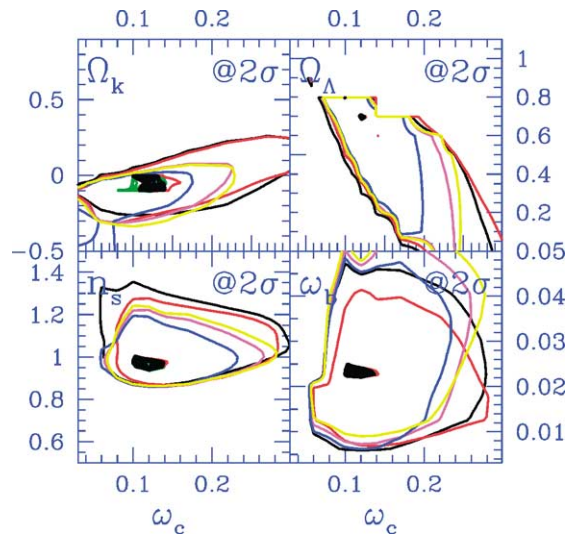


Fig. 6. Successive constraints in the $\Omega_k = 1 - \Omega$, Ω_Λ , n_s , $\omega_B = \Omega_B h^2$ versus $\omega_c = \Omega_{CDM} h^2$ cuts in the global parameter space fitted to the $C(\ell)$ successive data, using COBE/DMR in all cases. The colour coding is the following: CBI = black, VSA = (outer) red, Archeops = yellow, ACBAR = blue, Ruhl cut for Boomerang = magenta. Green corresponds to Acbar + Archeops + Ruhl + DASI + Maxima + VSA + CBI. The interior red is all of the above + WMAP with no prior on τ , while black is with a τ prior motivated by their ‘model independent’ result from the TE analysis (it is broader than a 0.16 ± 0.04 Gaussian). (Courtesy D. Bond.)

signs of inconsistencies. This was in fact in place before the WMAP results, but it is remarkable that adding WMAP essentially zooms-in to the expected values, bringing now further support to the model and its parameters, as recalled in Section 2.

This is quite an achievement already, although the CMB constraining power on the theoretical parameters is far from exhausted and a number of crucial predictions of the theory still remain to be checked. Many ground and balloon experiments will undoubtedly continue uncovering the properties of the polarised CMB emission (see Delabrouille et al., this issue). Planck should then definitely fix the temperature power spectrum, provide a very accurate view of the E polarisation, and might measure the B spectrum. Nevertheless a precise determination of the latter will probably have to await a next (fourth) generation satellite dedicated to the measurement of polarisation. In the process, we shall also learn more about astrophysical foregrounds, like clusters, IR galaxies and radio-sources, and the interstellar medium of our own Galaxy.

6. Conclusions

Measurements of the CMB are quite unique in the ensemble of astrophysical observations that are used to constrain cosmological models. They have the same character as fundamental physics experiments; they relate fundamental physical parameters describing our world to well specified signatures which can be predicted before hand with great accuracy.

The knowledge of CMB anisotropies has literally exploded in the last decade, since their momentous discovery in 1992 by the DMR experiment on the COBE satellite. Since then, the global shape of the spectrum has been uncovered thanks to many ground and balloon experiment and most recently the WMAP satellite, so far confirming the simplest inflationary model and helping shape our surprising view of the Universe: spatially flat, and dominated by dark energy (or Λ) and cold dark matter, with only a few per cent of atoms. However, the quest is far from over, with many predictions still awaiting to be checked and many parameters in need of better determination.

If the next 10 years are as fruitful as the past decade, many cosmological questions should be settled, from a precise determination of all cosmological parameters to the characteristics of the mechanism which seeded the growth of structures in our Universe, if something even more exciting than what is currently foreseen does not surge from the future data. . .

Acknowledgement

I am very grateful to D. Bond for providing up to date figures for the discussion.

References

- [1] R.A. Alpher, R. Herman, *Nature* 162 (1948) 774.
- [2] D.J. Fixsen, J.C. Mather, The spectral results of the far-infrared absolute spectrophotometer instrument on COBE, *Astrophys. J.* 581 (2002) 817–822.
- [3] C.L. Bennett, M. Halpern, G. Hinshaw, N. Jarosik, A. Kogut, M. Limon, S.S. Meyer, L. Page, D.N. Spergel, G.S. Tucker, E. Wollack, E.L. Wright, C. Barnes, M.R. Greason, R.S. Hill, E. Komatsu, M.R. Nolta, N. Odegard, H.V. Peiris, L. Verde, J.L. Weiland, First-year Wilkinson Microwave Anisotropy Probe (WMAP) observations: preliminary maps and basic results, *Astrophys. J. Supp.* 148 (2003) 1–27.
- [4] D.N. Spergel, L. Verde, H.V. Peiris, E. Komatsu, M.R. Nolta, C.L. Bennett, M. Halpern, G. Hinshaw, N. Jarosik, A. Kogut, M. Limon, S.S. Meyer, L. Page, G.S. Tucker, J.L. Weiland, E. Wollack, E.L. Wright, First-year Wilkinson Microwave Anisotropy Probe (WMAP) observations: determination of cosmological parameters, *Astrophys. J. Supp.* 148 (2003) 175–194.
- [5] R.K. Sachs, A.M. Wolfe, *Astrophys. J.* 147 (1967) 73.
- [6] W. Hu, CMB temperature and polarization anisotropy fundamentals, *Ann. Phys.* 303 (2003) 203–225.
- [7] M.J. Rees, D.W. Sciama, Large scale density inhomogeneities in the Universe, *Nature* 217 (1968) 511.
- [8] U. Seljak, Rees–Sciama effect in a cold dark matter Universe, *Astrophys. J.* 460 (1996) 549.
- [9] Y.B. Zel’dovich, R.A. Sunyaev, *Astrophys. Space Sci.* 4 (1969) 301.
- [10] R.A. Sunyaev, Y.B. Zel’dovich, Formation of clusters of galaxies; Protocluster fragmentation and intergalactic gas heating, *Astron. Astrophys.* 20 (1972) 189.
- [11] R.A. Sunyaev, I.B. Zel’dovich, The velocity of clusters of galaxies relative to the microwave background – the possibility of its measurement, *Mon. Not. R. Astron. Soc.* 190 (1980) 413–420.
- [12] J.P. Ostriker, E.T. Vishniac, Generation of microwave background fluctuations from nonlinear perturbations at the era of galaxy formation, *Astrophys. J. Lett.* 306 (1986) L51–L54.
- [13] E.T. Vishniac, Reionization and small-scale fluctuations in the microwave background, *Astrophys. J.* 322 (1987) 597–604.
- [14] S. Dodelson, J.M. Jubas, Reionization and its imprint of the cosmic microwave background, *Astrophys. J.* 439 (1995) 503–516.
- [15] W. Hu, M. White, CMB anisotropies in the weak coupling limit, *Astron. Astrophys.* 315 (1996) 33–39.
- [16] N. Aghanim, F.X. Désert, J.L. Puget, R. Gispert, Ionization by early quasars and cosmic microwave background anisotropies, *Astron. Astrophys.* 311 (1996) 1–11.
- [17] A. Gruzinov, W. Hu, Secondary cosmic microwave background anisotropies in a Universe reionized in patches, *Astrophys. J.* 508 (1998) 435–439.
- [18] S.R. Knox, L. Dodelson, D. Dodelson, *Phys. Rev. Lett.* 81 (1998).
- [19] N. Aghanim, F.X. Désert, J.L. Puget, R. Gispert, Erratum: Ionization by early quasars and cosmic microwave background anisotropies, *Astron. Astrophys.* 341 (1999) 640.
- [20] N. Aghanim, C. Balland, J. Silk, Sunyaev–Zel’dovich constraints from black hole-seeded proto-galaxies, *Astron. Astrophys.* 357 (2000) 1–6.
- [21] F. Pajot, Ph.D. thesis, Paris VII University.
- [22] M. Halpern, D. Scott, Future cosmic microwave background experiments, 1999, astro-ph/9904188.
- [23] C.H. Lineweaver, Inflation and the cosmic microwave background, in: *Proceedings of the New Cosmology Summer School, 2003*, astro-ph/0305179.